Journal of Organometallic Chemistry, 135 (1977) 281—299

VIBRATIONAL SPECTRA AND NORMAL COORDINATE ANALYSIS OF CF_3 COMPOUNDS

XIX *. MOLECULAR STRUCTURE AND VIBRATIONAL SPECTRA OF BIS(TRIFLUOROMETHYL)MERCURY, $(CF_3)_2Hg$

D.J. BRAUER, H. BÜRGER and R. EUJEN

Fachbereich 9, Anorganische Chemie, Gesamthochschule, 5600 Wuppertal (B.R.D.)

(Received February 24th, 1977)

Summary

The crystal structure of bis(trifluoromethyl)mercury has been determined from 116 absorption and extinction corrected X-ray data collected by counter methods. The compound crystallizes in the cubic space group T_h^6-$Pa3$ with a = 8.127(2) Å, Z = 4, d_c 4.19 and d_0 4.22 g cm^{-3}. Anisotropic refinement converged with a conventional R factor of 0.023. Crystals of $(CF_3)_2Hg$ consist of discrete monomeric molecules possessing $S_6(\bar{3})$ crystallographic symmetry. Thus the C—Hg—C fragment and the CF_3 groups must be linear and staggered respectively. The Hg—C and C—F bond lengths are 2.109(16) Å (corrected 2.118 Å) and 1.321(7) Å (corrected 1.349 Å), respectively, the distances being corrected for librational shortening. The Hg—C—F and F—C—F bond angles are 111.7(7)° and 107.2(7)°, respectively. Infrared and Raman spectra of $(CF_3)_2Hg$ gaseous, crystalline, and in solution were recorded and analyzed for D_{3d} molecular symmetry. In the solution spectra all fundamentals were observed. A quadratic GVFF yielded the stretching force constants f(HgC) 2.18 and f(CF) 5.15 mdyn Å^{-1}. In order to interpret the Raman spectrum of crystalline $(CF_3)_2Hg$ a factor group analysis was performed. Single crystals exhibit dynamical splittings ($\Delta\nu_i \leqslant 18$ cm^{-1}) of the molecular vibrational modes with "gerade" symmetry. The symmetry of the crystal vibrations was elucidated by single crystal Raman polarization measurements. Polarization data for solution Raman spectra were employed to calculate the relative intensities of the crystal components of the a_{1g} molecular modes.

---

* For part XVIII see ref. 1.

Introduction

Structural investigations of $E(CF_3)_n$ and $E(CH_3)_n$ compounds have shown that E—C(CF_3) bonds are longer than E—C(CH_3) bonds if the main group element E is more electropositive than carbon [2]. Similarly E—C stretching force constants are significantly smaller in those compounds (e.g. E = P, As [3], Ge [4,5], Sn, Pb [6]) than in the corresponding methyl analogs.

$(CF_3)_2Hg$ is one of the few known "binary" trifluoromethyl derivatives of an electropositive element. Along with its utility in chemical syntheses [7] $(CF_3)_2Hg$, which is both volatile and high melting (m.p. 163°C) [8], is therefore an attractive species for structural and spectroscopic investigations. Aside from its comparison with $(CH_3)_2Hg$ [9—11] the geometry and force constants of the CF_3 groups are of interest. They are predicted to be close to the weak bond end of the sequence ranging from CF_4 (r(CF) 1.320(8) Å [2], f(CF) 7.32 mdyn Å^{-1} [12]) to $CF_3BF_3^-$ (r(CF) 1.360(8) Å, f(CF) 4.85 mdyn Å^{-1} [13]).

A preliminary X-ray report on $(CF_3)_2Hg$ stated that the crystals are cubic and have four molecules in the unit cell. Although the space group was not mentioned, the C—Hg—C skeleton was reported to be linear [13]. Analysis of the Raman and infrared spectra of $(CF_3)_2Hg$ in various solvents implied inversion symmetry and revealed a lack of sensitivity of the molecule towards solvents and dissolved ions [14]. Since we found that the Raman spectrum of crystalline $(CF_3)_2Hg$ is more complex than the solution spectra, simultaneous X-ray and solid state vibrational spectroscopic investigations appeared to be particularly desirable. The results of these investigations are presented.

Experimental

Materials; Bis(trifluoromethyl)mercury was prepared by the decarboxylation of $(CF_3COO)_2Hg$ in the presence of K_2CO_3 [7,15] and purified by sublimation in vacuo. Single crystals were grown by slow sublimation at atmospheric pressure.

Spectra. Infrared spectra were recorded in the 4000—200 and 400—25 cm^{-1} region with Beckman IR 12 and Beckman FT 720 instruments, respectively, employing KBr or polyethylene windows. Sharp bands are believed to be accurate to ±0.5 cm^{-1} and are not vacuum corrected. Resolution is <2 cm^{-1} above 200 cm^{-1} and <0.6 cm^{-1} above 650 cm^{-1}. Gas phase spectra were recorded at ambient temperature (vapor pressure ca. 0.5 torr) employing 10 cm cells. Solution spectra were obtained from saturated solutions using films or 0.05 and 0.1 mm cells. The region below 200 cm^{-1} was examined as Nujol mulls.

Raman spectra of crystalline powder and of saturated solutions sealed in 1 mm glass capillaries were obtained with a Cary 82 spectrometer upon excitation with a Kr^+ laser (output 500 mW at 6471 Å). For single crystal studies octahedral specimens with ca. 1 mm edges were sealed in a conical capillary which was mounted on a goniometer head. Crystals were oriented optically with the crystal axes parallel to the incident laser beam and the direction of observation. Final alignment was achieved by optimization of the output signal and the depolarization ratio of the 1164 cm^{-1} line.

X-ray data collection. In order to prevent sublimation crystals were coated with vacuum grease before they were placed in thin-walled glass capillaries. The

space group and unit cell constants were determined directly on the diffractometer. Crystals belong to the cubic system. The systematic absences $hk0$ ($h = 2n + 1$), $h0l$ ($l = 2n + 1$) and $0kl$ ($k = 2n + 1$) are unique for the space group T_h^6-$Pa3$. The cell constant $a = 8.127(2)$ Å * was determined from 12 θ values (Mo-K_{α_1} λ 0.70926 Å, Mo-K_{α_2} λ 0.713543 Å, θ scans with thin-slit collimator, t 27°); d_c = 4.19 g cm^{-3} for $Z = 4$ agrees with the reported density, 4.22 g cm^{-3} [8].

The data crystal, which had a mean length along the threefold axes of 0.19 mm, was aligned with the 111 parallel to the Φ axis. The pulse height analyzer was set to receive all of the ZrO_2 filtered Mo-K_α radiation. ω scans of several strong, low order reflections gave symmetrical peaks with a full-width at half-height of 0.2°.

Intensity data hkl were collected by a five value $\theta - 2\theta$ scan technique [16]. The 2θ scan range (1.20—2.04°) was chosen from a function of the Bragg angle and was symmetric with respect to the θ (Mo-$K_{\bar{\alpha}}$) position. All hkl with $\theta < 18°$ were measured with 2θ scan speeds between 20 and 0.625° min^{-1}, about half of them being collected twice. Only reflections with hkl all even or all odd gave significant intensities for $\theta > 18°$; so reflections ($15° < \theta < 30°$) of these two parity groups were measured with a 2θ scan speed of 2.5° min^{-1}. The total number of reflections is 527.

The intensity of the standard reflection, $02\bar{2}$, which was monitored in periods of 40 reflections, increased about 20% during data collection. That this behaviour was not typical for the whole data set was revealed by remeasurement of other reflections. The data were corrected for Lorentz and polarization effects (Lp) and absorption (μ(Mo-K$_\alpha$) = 287.12 cm^{-1}) **. The transmission factor A varied from 0.021 to 0.082. The absorption correction accounted for the variation in the intensity of the 111, which was measured at 14 different Φ values. Estimated standard deviations were calculated from the formula $\sigma^2(|F_o|) = [\sigma^2(I) + (0.05\ I)^2]/2|F_o|LpA$, where $\sigma(I)$ is determined from counting statistics [16]. Averaging of equivalent data yielded 119 unique reflections, of which three had $|F_o| < 2\sigma(|F_o|)$.

Solution and refinement of the structure

The structure was solved by Patterson methods. The location of the Hg atom on a S_6 ($\bar{3}$) symmetry site was confirmed, and the C atom was found on the threefold axis. The structure was refined by least-squares methods. The function minimized was $\Sigma w\Delta^2$, where $w = 1/\sigma(|F_o|)^2$ for $|F_o| \geqslant 2\sigma(|F_o|)$, otherwise $w = 0$ and $\Delta = ||F_o| - |F_c||$. Relativistic neutral atom scattering factors [17], corrected for real and imaginary anomalous dispersion [18], were used for all atoms. Isotropic refinement reduced $R = \Sigma\Delta/\Sigma|F_o|$ and $Rw = [\Sigma w\Delta^2/\Sigma w|F_o|^2]^{1/2}$ to 0.080 and 0.083, respectively. Anisotropic refinement converged (R = 0.047 and Rw

---

* Unless another meaning is clearly specified, a number in parentheses following a numerical value is the estimated standard deviation in the last digit.

** In addition to local programs for the CDC 7600/7200, the programs were modified versions of Sheldrick's SHEL-X package for absorption correction, least-squares, Fouriers and molecular dimensions, of Roberts and Sheldrick's XANADU for the thermal motion calculation, of Johnsons ORTEP for the drawing and of DJB's REDUCE and ABWINK for data reduction and intermolecular distances respectively.

TABLE 1

POSITIONAL AND THERMAL PARAMETERS FOR $(CF_3)_2Hg$

Atom	x	y	z	U_{11} [a,b]	U_{22}	U_{33}	U_{12}	U_{13}	U_{23}
Hg	0.0	0.0	0.0	0.0323(3)	0.0323(3)	0.0323(3)	−0.0021(3)	−0.0021(3)	−0.0021(3)
C	0.1499(11)	0.1499(11)	0.1499(11)	0.037(4)	0.037(4)	0.037(4)	−0.006(4)	−0.006(4)	−0.006(4)
F	0.0818(8)	0.2951(7)	0.1766(9)	0.070(5)	0.042(3)	0.101(5)	−0.001(4)	−0.017(5)	−0.027(4)

[a] The form of the anisotropic thermal ellipsoid is: $\exp[-2\pi^2(h^2a^{*2}U_{11} + k^2b^{*2}U_{22} + l^2c^{*2}U_{33} + 2hka^*b^*U_{12} + 2hla^*c^*U_{13} + 2klb^*c^*U_{23})]$. [b] The root-mean-square displacements of the atoms along their principal axes are: Hg, 0.168, 0.186, 0.186 Å; C, 0.16, 0.21, 0.21 Å; F, 0.17, 0.26, 0.34 Å.

TABLE 2

SELECTED INTERATOMIC DISTANCES (Å) AND BOND ANGLES (°) IN $(CF_3)_2Hg$

Distance			Angle	
Hg—C	2.109(16)	2.118(16) [a]	C—Hg—C″	180
C—F	1.321(7)	1.349(8) [a]	Hg—C—F	111.7(7)
Hg—F′ [b]	3.181(7)		F—C—F‴	107.2(7)

[a] This distance is corrected for librational motion. [b] Coordinates r of primed atoms are related to those in the asymmetric unit as follows: $r' = -x, y-0.5, 0.5-z; r'' = -x, -y, -z; r''' = z, x, y$.

= 0.069) with physically impossible thermal parameters for the C atom. Examination of an $|F_0|, F_c$ list revealed a possible extinction effect. With an extinction correction of the type $|F_c|^* = |F_c|(1 - x|F_c|^2/\sin\theta)$, six cycles of refinement converged with $R = 0.023$ and $Rw = 0.026$. Physically possible thermal parameters were obtained for all atoms.

On the final cycle all parameter shifts were less than 2% of their standard deviations. The value of x is $3.0(1) \times 10^{-7}\ e^{-2}$. The largest extinction correction was applied to $|F_c|$ of the 111, 32%. Plots of a function of $\langle w\Delta^2\rangle^{1/2}$ versus the parity groups, Miller indices, $\sin\theta/\lambda$ and $|F_0|$ were reasonably flat, thus confirming the relative validity of the weighting scheme. The residual density on the final difference Fourier map never exceeded 0.5 e Å^{-3}, which may be compared with the height of a carbon atom in this structure, 9.5 eÅ^{-3}. Positional and thermal parameters are given in Table 1. The labelling is shown in Fig. 1. Distances and angles are given in Table 2, correlation between refined parameters being used only in the calculation of errors in molecular parameters *.

The temperature factors were investigated for rigid body thermal motion [19]. The error of fit, 0.006 Å^2, compares well with the root-mean-square (rms) error in the thermal parameters, 0.004 Å^2. The translational tensor is essentially isotropic with rms amplitudes of 0.18(2) Å and 0.16(1) Å parallel and perpendicular to the C_3 axis respectively. The librational tensor is anisotropic, the rms libration about the C_3 axis, 11.9(3)°, being greater than that about axes perpendicular to this direction, 3.8(6)°. This motion is not unreasonable for an elongated aspherical top such as $(CF_3)_2Hg$. So librational corrections were applied to the Hg—C and C—F bond lengths [20] (Table 2).

Description of the structure

A unit cell drawing is presented in Fig. 1. $(CF_3)_2Hg$ crystallizes as monomeric molecules of S_6 ($\bar{3}$) crystallographic symmetry. The shortest intermolecular F—F contact, 3.145(9) Å, is much longer than twice the Van der Waals radius of a F atom, 2.94 Å [21]. Apparently intermolecular F—F interactions contribute little to the packing forces. Six intermolecular Hg—F contacts of 3.181(7) Å are formed per Hg atom. The importance of these contacts is debatable since the Hg atom has unfilled 6p orbitals available for bonding. However the distances

* A $|F_0|, F_c$ list is available from D.J.B.

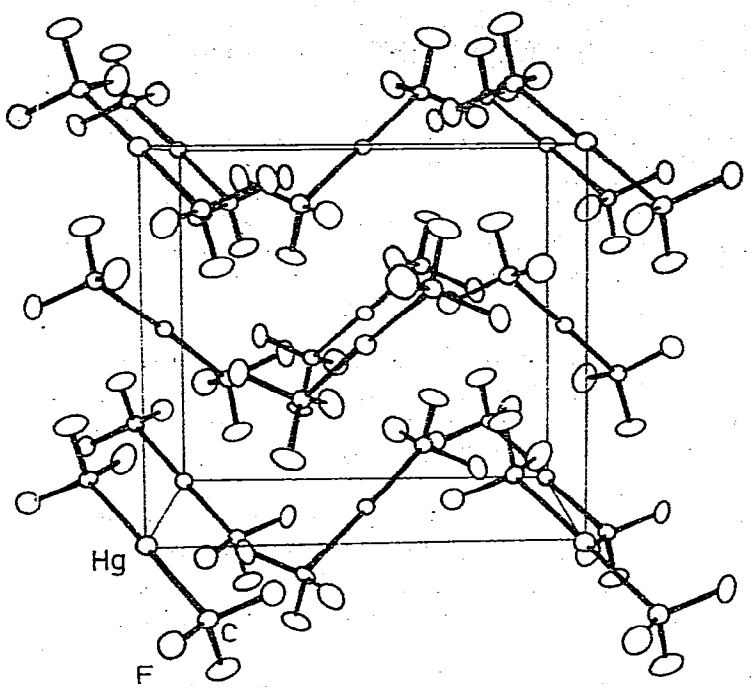

Fig. 1. Perspective drawing of the $(CF_3)_2Hg$ unit cell with 20% probability thermal ellipsoids.

are very long compared to those in HgF_2, 2.46 Å [22], and Hg_2F_2, 2.31 and 2.70 Å [23]. The $(CF_3)_2Hg$ intramolecular Hg—F contact is also much shorter, 2.873(6) Å.

Lowering the symmetry of $(CF_3)_2Hg$ from D_{3d} ($\bar{3}m$) to S_6 ($\bar{3}$) releases constraints on the molecular vibrations (see below) but not on the molecular structure. The Hg—C bond length, 2.109(16) Å (corrected 2.118 Å), lies on the long end of the range of Hg—C(CH_3) distances found in CH_3HgCl, r_s 2.061 ± 0.020 Å [24], CH_3HgBr, r_s 2.074 ± 0.015 Å [24], CH_3HgCN, 2.08(2) Å [25] and $(CH_3)_2Hg$, r_g 2.083 ± 0.005 Å [10] and r_0 2.094 ± 0.005 Å [9]. The spread in these Hg—C bond lengths is not much more than three of our standard deviations.

Using the linear C—F bond length/F—C—F bond angle dependence [2], we calculate a C—F distance of 1.342 Å from the observed F—C—F angle of 107.2(7)°. The calculated value is in better agreement with the corrected C—F distance, 1.349 Å, than with the uncorrected value, 1.321(7) Å. This agreement adds credence to our corrected values of the bond lengths. A C—F distance near 1.35 Å appears to be typical of CF_3 compounds of electropositive elements; e.g., in $K[CF_3BF_3]$, corrected C—F = 1.360(8) Å [12], in $\{\eta\text{-}(CH_3C)_4(CF_3)Pt[(PC_6H_5)(CH_3)_2]_2\}PF_6$, C—F = 1.36 Å [26] and in $\eta\text{-}C_5H_5(CF_3)Ni[P(C_6H_5)_3]_2$, C—F = 1.35 Å [27].

Vibrational spectra

Solution and gas phase spectra. The infrared and Raman spectra of bis(trifluoromethyl)mercury in solution (and in the gas phase) can be analyzed assum-

TABLE 3

DISTRIBUTION OF MOLECULAR VIBRATIONS IN $Hg(CF_3)_2$

	a_{1g} (Ra, p)	a_{2g} (—)	e_g (Ra)	a_{1u} (—)	a_{2u} (IR)	e_u (IR)
$\nu_{as}(CF_3)$			ν_4			ν_{11}
$\nu_s(CF_3)$	ν_1				ν_8	
$\delta_{as}(CF_3)$			ν_5			ν_{12}
$\delta_s(CF_3)$	ν_2				ν_9	
$\rho(CF_3)$			ν_6			ν_{13}
$\nu(HgC)$	ν_3				ν_{10}	
$\delta(HgC_2)$						ν_{14}
Torsion				ν_7		

ing D_{3d} symmetry as determined by the X-ray analysis. The approximate description of the vibrational modes, their symmetry and the selection rules are given in Table 3. The Raman spectrum of $(CF_3)_2Hg$ dissolved in acetonitrile is reproduced in Fig. 2a. Infrared and Raman frequencies are listed in Table 4.

We agree with the assignments given by Downs [14] with the following exceptions:

1. The assignments of $\nu_s(CF_3)$ and $\nu_{as}(CF_3)$ have to be reversed. Polarization measurements in different solvents clearly indicate that the line near 1155 cm^{-1} is polarized ($\rho = 0.56 \pm 0.03$) whereas the weak, broad feature close to 1060 cm^{-1} is depolarized ($\rho = 0.77 \pm 0.05$). This assignment is supported by

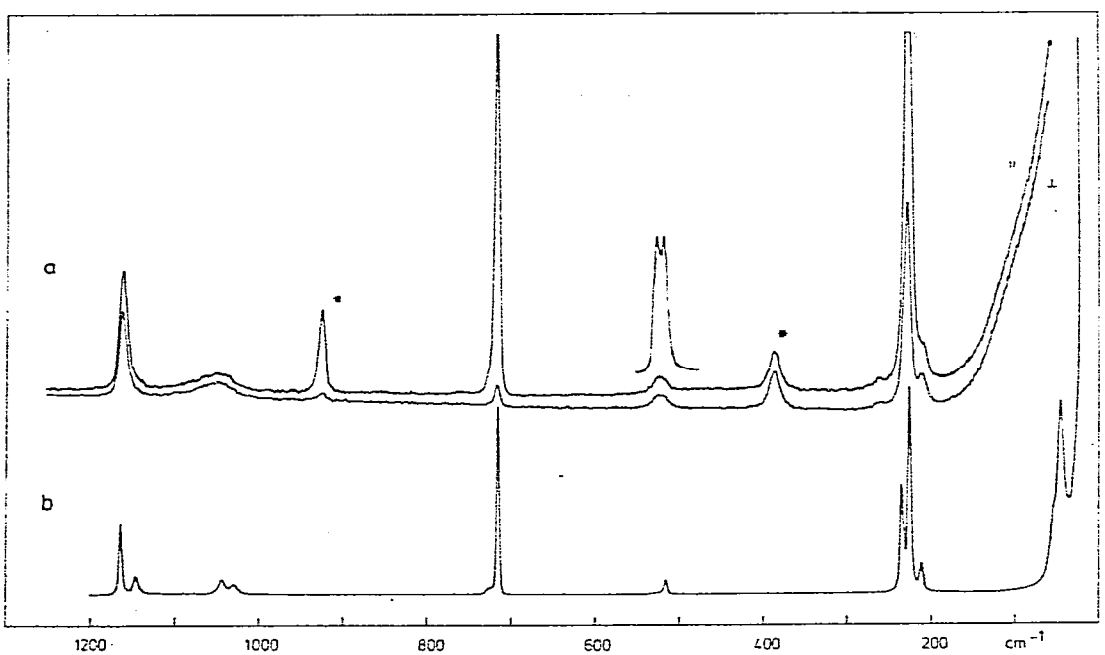

Fig. 2. Raman spectra of $(CF_3)_2Hg$: (a) Polarization spectra in acetonitrile solution. Lines marked with an asterisk are due to the solvent; (b) crystal powder spectrum.

TABLE 4

INFRARED AND RAMAN SPECTRA OF $(CF_3)_2Hg$ (cm^{-1})

IR gas	IR, solution		Raman, solution			Raman solid	I^a	ρ^b	Assignment
	C_6H_6	CH_3CN	C_6H_6	CH_3CN	H_2O				
	32m [c]								(ν_{trans})
						46s 52(sh)			ν_{lib}
	68s [c]								ν_{14}
			205	209	211	211m	4	dp	ν_6
			224	226.5	228	224vs	100	0.23 ± 0.02	ν_3
			(226) [e]			234s		(0.18)	
(258?)	259	261m		261			≪1		ν_{13}
274	271	272s							ν_{10}
			(515sh)	518	517	516w			
			525	525		527(sh)	2	0.70 ± 0.10	$\nu_5/2\nu_{13}$
	(528vw)	521w							ν_{12}
			715	713	713	714vs	55	0.03 ± 0.01	ν_2
			(719 [e])			725(sh)		(0.03)	$\nu_5 + \nu_6$
	716	713m							ν_9
	(728(sh))	723w							$\nu_6 + \nu_{12}$
			1065	1051	1050	1030w-m 1043m	2	0.77 ± 0.05	ν_4
1116	1083	1070vs							
	(1095 [a])	(1069 [d])							ν_{11}
1143	1135	1145vs							
	(1135 [e])	(1147 [d])							ν_8
			1150	1159	1159	1146 1163s	16	0.56 ± 0.03	ν_1
								(0.61)	

[a] Relative intensities in acetonitrile solution, not corrected for spectral sensitivity. [b] Depolarization ratio in acetonitrile solutions, values in parentheses refer to C_6H_6 solution. [c] Nujol mull. [d] Aqueous solution. [e] Cyclohexane solution.

intensity arguments, $\nu_s(CF_3)$ is usually stronger than $\nu_{as}(CF_3)$ in the Raman effect, and the pronounced environmental dependence of the bands close to 1060 cm^{-1}. Furthermore the crystal spectrum (see below) can only be analyzed when the assignment of ν_s and $\nu_{as}(CF_3)$ is reversed.

2. The CF_3 rocking modes are assigned to the infrared band at 259 cm^{-1} (ν_{13}) and the Raman line at 205 cm^{-1} (ν_6) observed in C_6H_6 solution. We also observed a very weak Raman band at 261 cm^{-1} which was formerly [14] assigned to ν_6. However, we attribute this feature to ν_{13}, though its coincidence with the infrared band suggests that the mutual exclusion principle is violated due to the anharmonicity of the large rocking amplitude. Since all solution Raman spectra reveal a depolarized line between 205 and 211 cm^{-1}, its assignment to ν_6 is beyond any doubt. A difference of ca. 50 cm^{-1} between the two rocking modes has similarly been reported for $(CH_3)_2M$ molecules [11,28].

3. A new, rather strong absorption in the far infrared at 68 cm^{-1} is assigned to the skeletal bend ν_{14}.

4. The infrared spectra of KBr or CsBr pellets are more complex than expected for D_{3d} symmetry, frequencies and band contours varying in an irreproducible manner, especially in the ν(CF) region. This region comprises two groups of frequencies occurring at 1040 to 1070 and 1130 to 1165 cm^{-1}, respectively.

The infrared spectra of KBr pellets can be roughly regarded as a superposition of two spectra (I, II) with varying relative intensities (Table 5). Raman studies of KBr pellets or even KBr mulls prove that the single crystal behaviour is no longer retained. The spectra are likely to originate from crystalline fragments imbedded in host material. Observation of the "Raman forbidden" vibrations ν_{10} and ν_{13} indicates removal of the inversion center.

Solvent effects of the Raman lines associated with ν_1 to ν_3 have been studied previously [14]. More significant shifts are however observed for nonsymmetric vibrations. The gas phase IR frequencies of ν_8 ($\nu_s(CF_3)$) and ν_{11} ($\nu_{as}(CF_3)$) are lowered in nonpolar solvents (e.g. benzene) by 8 and 33 cm^{-1} respectively. Increasing polarity of the solvent (water or acetonitrile) leads to small, but significant increase of the $\nu_s(CF_3)$ (~10 cm^{-1}), $\rho(CF_3)$ (3—6 cm^{-1}) and $\nu(HgC_2)$ (1—4 cm^{-1}) frequencies whereas ν_{as}, δ_s and $\delta_{as}(CF_3)$ decrease by 15, 2 and ca. 8 cm^{-1}, respectively. The averaged crystal frequencies as well as the frequencies of KBr or CsBr pellets correlate with the spectra in polar solvents. The shifts which appear upon increasing the polarity of the medium from nonpolar, like in the gas phase, to maximum polarity can be reproduced qualitatively with

TABLE 5

INFRARED AND RAMAN FREQUENCIES IN THE CF STRETCHING REGION (cm^{-1})

IR: KBr pellet		IR: CsBr pellet	Raman in KBr		Raman crystalline	
I	II		mull	pellet		
	995m		1000w	995w		$(\nu_{10} + \nu_2/\nu_9)$
1043s		1045vs	(1030vw)	1027w	1029w	
	1068s		(1080vw)	1075m	1044w	$\nu_{as}(CF_3)$
1148vs	1139vs	1133	1135w	1146w	1146w	
(1165m)	1161s	1148 vs	1174s	1164s	1164s	$\nu_s(CF_3)$

simple force constant calculations for a CF_3X model (X being a heavy atom) assuming that (a) the FCF angle decreases by about 1°, (b) the CF bond lengthens slightly (about 0.01 Å) and (c) the CF stretching force constant decreases by 3 to 5%.

The angle/bond length behaviour agrees with the general relationship for fluoroalkyl compounds given by Bauer et al. [2]. From the crystal data it can be predicted that the geometry of the CF_3 groups in gaseous $(CF_3)_2Hg$ is very close to that of other CF_3 compounds [2] (angle FCF ~108°, r(CF) ~1.34 Å).

The solvent dependency of frequencies helps to detect an anharmonic resonance of ν_5 with $2\nu_{13}(E_g)$. The shape of the Raman spectrum near 520 cm^{-1} is governed by a crossover of two frequencies. Increasing polarity of the solvent shifts ν_5 to lower and $2\nu_{13}$ to higher wavenumbers. An equal intensity doublet is observed in CH_3CN solution, whereas in benzene ν_5 ($\delta_{as}(CF_3)$) exhibits only a shoulder at lower frequency. In aqueous solution ν_5 falls below $2\nu_{13}$.

A further splitting attributable to Fermi resonance is observed with polar solvents such as acetonitrile or diethyl ether in which ν_9 ($\delta_s(CF_3)$) may interact with the A_{2u} component of $\nu_6 + \nu_{12}$. In benzene solution however ν_9 and the sum of ν_6 and ν_{12} are further apart. The intensity of the combination band $\nu_6 + \nu_{12}$ decreases due to weakening of the $\nu_9/(\nu_6 + \nu_{12})$ resonance such that it appears only as a weak shoulder of ν_9.

Crystal Spectra. The Raman spectrum of $Hg(CF_3)_2$ as crystalline powder is shown in Fig. 2b. Frequencies are listed in Table 4. Due to their excellent quality the single crystal Raman spectra permitted the observation of several combination bands. The powder Raman spectra reveal that: (1) ν_s, $\nu_{as}(CF_3)$ and $\nu_s(HgC_2)$ split into two components, (2) a new, intense band with a shoulder at higher frequency is observed around 45 cm^{-1}, and (3) the principle of mutual exclusion concerning centro-symmetric molecules is obeyed throughout, no "ungerade" vibrations appearing in the Raman effect.

Factor group analysis

The cubic unit cell contains four molecules which occupy S_6 sites. The selection rules interrelating molecular symmetry (D_{3d}), site symmetry (S_6) and crystal symmetry (T_h^6) are given in Table 6. The inversion center is retained throughout. The nondegenerate vibrations of the free molecule transform under crystal symmetry into one a and one f component whereas one e and two f modes result from the degenerate vibrations. The optical translational modes transform according to $\Gamma_{trans} = a_u + e_u + 2f_u$, whereas the Raman active vibrations comprise $\Gamma_{lib} = a_g + e_g + 3f_g$, the a_g and one f_g mode resulting from rotation about the molecular C_3 axis. The crystal modes can be assigned to symmetry species with the aid of single crystal polarization data. If the incident laser beam along the y axis is polarized in the xy plane, the Raman scattering observed in the z direction may be polarized either in the xz (∥) or in the yz (⊥) direction, the respective notation being $y(xx)z$ and $y(xy)z$. The intensity of the Raman scattering with the appropriate polarization properties is directly proportional to α_{xx}^2 and α_{xy}^2 respectively. Under T_h symmetry the elements of the polarizability tensor α transform to $(\alpha_{xx} + \alpha_{yy} + \alpha_{zz})$ for a_g and $(\alpha_{xx} + \alpha_{yy} - 2\alpha_{zz}, \alpha_{xx} - \alpha_{yy})$ for e_g, whereas the off-diagonal elements $\alpha_{xy}, \alpha_{xz}, \alpha_{yz}$ are of f_g symmetry.

The a_g modes are easily detected because their depolarization ratios $I(\perp)/I(\parallel)$

TABLE 6

Symmetry correlations for molecular and crystalline $(CF_3)_2Hg$

D_{3d} (molecule)	S_6 (crystal site)	T_h (unit cell)
a_{1g}	a_g	a_g (Ra)
a_{2g}		f_g (Ra)
e_g	e_g	e_g (Ra)
		$2f_g$ (Ra)
a_{1u}	a_u	a_u
a_{2u}		f_u (IR)
e_u	e_u	e_u
		$2f_u$ (IR)

are zero, irrespective of the crystal orientation. If irradiation and observation are parallel to the crystallographic axes, only a_g and e_g modes are observed when the analyzer is adjusted parallel, while the intensity of the f_g vibration should be greatest for $y(xy)z$ ($\perp$) orientation of the analyzer. Rotation of the crystal by 45° about the z axis permits further distinction of a_g and e_g vibrations. Angular transformation of the tensor α leads to the new elements $\alpha_{x'x'} = 1/2(\alpha_{xx} + \alpha_{yy}) - \alpha_{xy}$ and $\alpha_{x'y'} = 1/2(\alpha_{xx} - \alpha_{xy})$. Now $\alpha_{x'x'}$ ($\parallel$) comprises both a_g and f_g components whereas e_g vibrations are expected to appear for perpendicular ($\perp$) orientation only.

Figure 3 reproduces the results for vibrations exhibiting crystal field splitting ($\nu_s(CF_3)$, $\nu_{as}(CF_3)$, and $\nu_s(HgC_2)$). Complete suppression of the inactive components could not be achieved, however, due to irregularities of the irradiated surface (octahedral edges) and, to a minor extent, due to misalignment of the crystal. From Fig. 3 it is evident that both doublets near 1150 and 230 cm^{-1} consist of a_g and f_g components, the latter being at higher wavenumbers. Consequently, their assignment to molecular a_{1g} modes (Table 6) is certain. The two bands at 1030 and 1043 cm^{-1} are of e_g and f_g symmetry, respectively. No further splitting of the 1043 cm^{-1} band due to its two f_g components was observed.

Since the rotation about the molecular C_3 axis is not likely to induce a large change of the crystal polarizibility, the librations at about 40—50 cm^{-1} are expected to belong to e_g or f_g symmetry. Indeed from a non-oriented single crystal no evidence could be gathered for a a_g mode. Due to the inferior quality of the oriented crystal spectra and overlap, a distinction of e_g and f_g modes was, however, not possible. The CF_3 rocking vibration at 211 cm^{-1} is almost insentitive to polarization measurements and thus consists of e_g and f_g components of about equal intensities. While $\delta_{as}(CF_3)$ reveals more pronounced f_g character, the Raman scattering associated with $\delta_s(CF_3)$ is almost entirely of a_g sym-

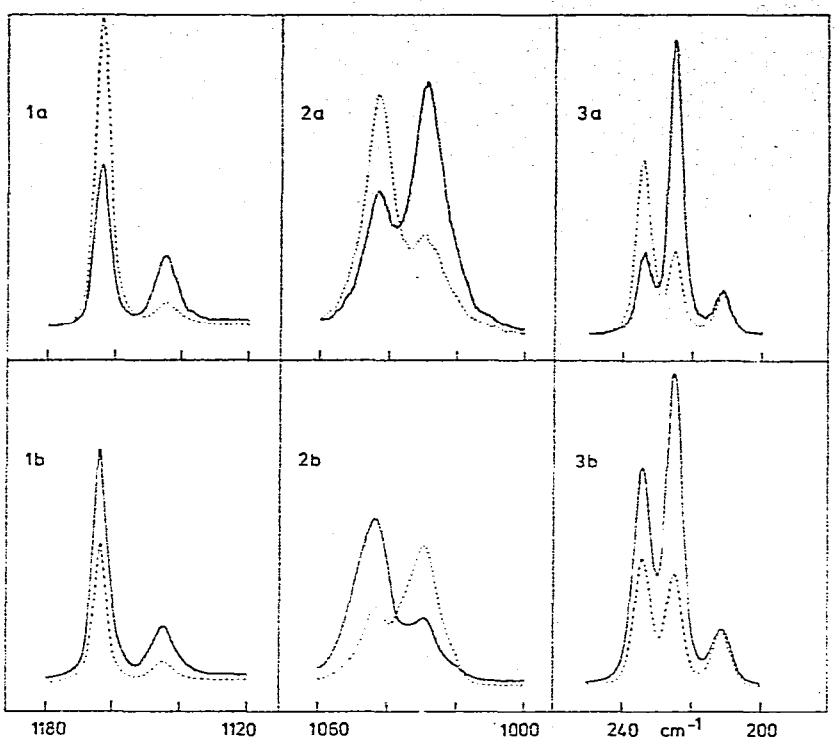

Fig. 3. Single crystal Raman spectra of $\nu_s(CF_3)$ (1), $\nu_{as}(CF_3)$ (2) and $\nu_s(HgC_2)/\rho(CF_3)$ (3). (a) Spectra with irradiation along the y axis and observation along the z axis; (b) spectra following 45° rotation about the z axis. Full lines represent parallel ($y(xx)z$), dotted lines vertical ($y(xy)z$) orientation of the analyzer.

metry. The relative Raman intensities of the crystal components of the molecular vibrations may be calculated from the elements of the molecular polarizability tensor if additivity of polarizabilities is assumed (oriented-gas model) [29]. In the crystal the relation of a_g to f_g intensity of modes emerging from molecular a_{1g} vibrations can be evaluated from the depolarization ratio ρ as determined on solution. The polarizability tensor $\alpha_k = \partial\alpha/\partial Q_k$ of the ith molecule ($i = 1$—4) is transformed from internal molecular coordinates (u, v, w) to crystal-fixed coordinates (x,y,z) according to eq. 1.

$$\alpha_{ki} = \tilde{T}_i \alpha_k T_i \tag{1}$$

The direction-cosine matrix T_i, e.g.

$$T_1 = \begin{bmatrix} u_x u_y u_z \\ v_x v_y v_z \\ w_x w_y w_z \end{bmatrix} = \begin{bmatrix} -0.789 & 0.211 & 0.577 \\ 0.211 & -0.789 & 0.577 \\ 0.577 & 0.577 & 0.577 \end{bmatrix}$$

reflects the orientation of the ith molecule in the unit cell. T_2, T_3 and T_4 are generated by 180° rotation about the x, y and z axis, respectively. Symmetry

transformation yields the crystal polarizabilities, e.g.

$$\alpha_k^c = U\alpha_{ki} \tag{2}$$

$$\alpha_k^c(a_g) = 1/2(\alpha_{k1} + \alpha_{k2} + \alpha_{k3} + \alpha_{k4}) \tag{3a}$$

and for one f_g component

$$\alpha_k^c(f_g^{\alpha}) = 1/2\sqrt{3}(3\alpha_{k1} - \alpha_{k2} - \alpha_{k3} - \alpha_{k4}) \tag{3b}$$

For cubic symmetry only α_{xx} and α_{xy} have to be calculated (the subscript k is omitted in the following):

$$a_g: \quad \alpha_{xx} = 2/3(\alpha_{uu} + \alpha_{vv} + \alpha_{ww}) - 2/3(\alpha_{uv} + \alpha_{uw} + \alpha_{vw}) \tag{4a}$$

$$\alpha_{xy} = 0 \tag{4b}$$

$$f_g: \quad \alpha_{xx} = 0 \tag{4c}$$

$$\alpha_{xy} = 1/3\sqrt{3}(2\alpha_{ww} - \alpha_{uu} - \alpha_{vv}) + 2/3\sqrt{3}(2\alpha_{uv} - \alpha_{uw} - \alpha_{vw}) \tag{4d}$$

For a_{1g} modes

$$\alpha_{uv} = \alpha_{uw} = \alpha_{vw} = 0 \tag{5a}$$

$$\alpha_{uu} = \alpha_{vv} = \alpha(\perp) \tag{5b}$$

$$\alpha_{ww} = \alpha(\parallel) \tag{5c}$$

Introducing the ratio $\alpha(\perp)/\alpha(\parallel) = q$ transforms eqns. 4a to 4d as follows:

$$a_g: \quad \alpha_{xx} = 2/3(2q + 1)\alpha(\parallel)$$

$$\alpha_{xy} = 0 \tag{6}$$

$$f_g: \quad \alpha_{xx} = 0$$

$$\alpha_{xy} = 2/3\sqrt{3}(1 - q)\alpha(\parallel)$$

Since the Raman intensities I are proportional to α^2, the ratio $I(a_g)/I(f_g)$, taking into account the triple degeneracy of the f mode, is calculated to be

$$I(a_g)/I(f_g) = (1 + 2q)^2/(1 - q)^2 \tag{7}$$

The q values of the a_{1g} vibrations ν_1 to ν_3 are obtained from the appropriate depolarization ratios ρ according to

$$q = \alpha(\perp)/\alpha(\parallel) = (1 + 2\rho \pm \sqrt{5\rho(3 - 4\rho)})(1 - 8\rho)^{-1} \tag{8}$$

This relation is reproduced by Fig. 4.

The appropriate sign of the root in eqn. 8 is determined from an estimation of the atomic displacements Q_k:

ν_1 ($\nu_s(CF_3)$): $|\alpha(\parallel)| > |\alpha(\perp)|$

ν_2 ($\delta_s(CF_3)$): $|\alpha(\perp)| > |\alpha(\parallel)|$

ν_3 ($\nu_s(HgC_2)$): $|\alpha(\parallel)| > |\alpha(\perp)|$

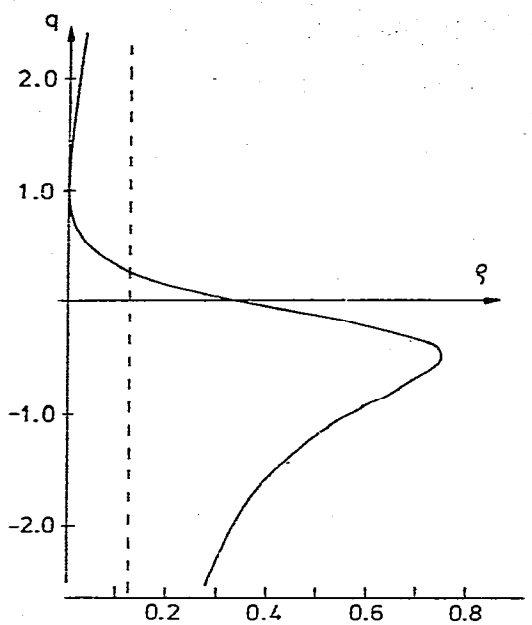

Fig. 4. Correlation for symmetric tops between the depolarization ratio ρ and the ratio of polarizabilities $q = \alpha_{y:x}/\alpha_{zz}$.

The comparison of the calculated and observed intensity ratios (Table 7) proves the validity of the above considerations and the nearly ideal behaviour of the $Hg(CF_3)_2$ molecule in this respect.

Normal coordinate analysis

In order to obtain further insight into the bonding and to describe quantitatively the vibrational properties of the $Hg(CF_3)_2$ molecule, a normal coordinate analysis following Wilson's FG matrix method was performed. The G matrix was calculated [30] from the geometry, determined by the X-ray analysis, employing the usual set of symmetry coordinates for two tops with C_3 symmetry. A starting force field was obtained according to the quadratic local symmetry

TABLE 7

CALCULATED AND OBSERVED INTENSITY RELATIONS FOR CRYSTAL COMPONENTS OF a_{1g} VIBRATIONS

	ρ	q	$I(a_g)/I(f_g)$ (found (calcd.))	$\nu(a_g)/\nu(f_g)$ (cm^{-1})
ν_1	0.56	—0.19	0.25 (0.27)	224/234
ν_2	0.03	2.25	>10 (19)	714/714
ν_3	0.23	0.10	1.7 (1.8)	1146/1164

TABLE 8

NONZERO SYMMETRY FORCE CONSTANTS (mdyn/Å) OF $(CF_3)_2Hg$, SCALED TO 1.000 Å

F_{ij}, ij =		F_{ij}, ij =	
11 = 88	6.78	12 = 89	0.65
22 = 99	1.68	13 = 810	0.12
33	2.38	23 = 910	−0.25
1010	1.98		
44 = 1111	4.33	45 = 1112	−0.50
55 = 1212	1.61	46 = 1113	0.50
66	0.53	56 = 1213	−0.10
1313	0.67	1314	0.05
1414	0.50		

force field principle [31] by transfer of force constants from HCF_3 [32] and $Hg(CH_3)_2$ [11] and refined to fit the fundamental frequencies obtained from solution spectra in benzene. The final nonzero symmetry force constants are listed in Table 8. Experimental and calculated fundamental frequencies together with the potential energy distribution in terms of diagonal force constants are given in Table 9. Significant mixing of vibrational character is restricted to the symmetric CF_3 stretching and bending (umbrella) vibrations. In all other vibrations of $Hg(CF_3)_2$ one single symmetry coordinate predominates. This behaviour contrasts that of many other CF_3 compounds studied so far and is mainly due to the comparatively heavy mercury atom. In Table 10 some inner force constants of $Hg(CF_3)_2$ are compared with those of CF_3HgCH_3 [33], $Hg(CH_3)_2$ [11] and other selected trifluoromethyl compounds.

TABLE 9

OBSERVED AND CALCULATED VIBRATIONAL FREQUENCIES (cm^{-1}) OF $Hg(CF_3)_2$, AND POTENTIAL ENERGY DISTRIBUTION $V(k)$ [a]

	ν_i; i =	Found	Calcd.	$V(k)$
a_{1g}	1	1150	1152	58(1), 54(2), 20(3)
	2	715	716	44(1), 37(2), 6(3)
	3	224	224	76(3), 5(2)
e_g	4	1066	1065	101(4), 25(5)
	5	525	524	76(5), 11(4)
	6	205	206	109(6)
a_{2u}	8	1135	1134	61(8), 54(9), 17(10)
	9	716	713	42(8), 40(9), 6(10)
	10	271	271	79(10), 12(9)
e_u	11	1083	1084	98(11), 24(12)
	12	525	526	73(12), 12(11)
	13	258	257	88(13), 8(14), 7(12)
	14	68	68	90(14), 17(13)

[a] $V(k) = F_{dia} \cdot L_{ik}^2 \cdot 100/\Sigma_{ij} F_{ij} \cdot L_{ik} \cdot L_{jk}$ for $V(k) > 5$.

TABLE 10

INNER FORCE CONSTANTS [a] AND BOND DISTANCES IN SELECTED TRIFLUOROMETHYL DERIVATIVES AND RELATED COMPOUNDS

	$(CF_3)_2Hg$	CF_3HgCH_3 [b]	$Hg(CH_3)_2$ [c]	$(CF_3)_3P$ [d]	$(CH_3)_3P$ [e]	$K[CF_3BF_3]$ [f]	HCF_3 [g]
f_r	5.15	4.89		6.0		4.85	6.48
$f_{rr'}$	0.82	0.84		0.846		0.90	0.82
r (Å)	1.349			1.340		1.360	1.334 [h]
f_R	2.18	2.06($Hg-CF_3$) 2.60($Hg-CH_3$)	2.38	2.6	2.91	3.63(3.64)	
f_{RR}	0.20	0.05	0.03	0.137	−0.03		
R (Å)	2.118		2.094 [i] 2.083 [k]	1.904	1.846 [l]	1.640(1.578)	
f_ζ	0.50	0.48	0.464				

[a] In mdyn/Å, r = C—F bond, R = E—C bond, ζ = CEC angle, f_ζ is scaled to 1 Å. [b] Ref. 33. [c] Ref. 11. [d] Ref. 34. [e] Ref. 35. [f] Ref. 13, values in parentheses are for $B(CH_3)_3$. [g] Ref. 36. [h] Ref. 2. [i] Ref. 9. [k] Ref. 10. [l] Ref. 38.

Discussion

Crystals of $(CF_3)_2Hg$ contain discrete centrosymmetric molecules. Presumably, weak intermolecular bonding occurs via the six 3.181(7) Å F—Hg interactions per Hg atom. Although this distance is long (vide supra), interactions between nonbonding fluorine 2*p* orbitals and unfilled mercury 6*p* orbitals and/or coulombic attraction between the oppositely charged F and Hg atoms appear to be significant. This bonding is reflected in the relatively high melting point of 163° [8]. The observed dynamic splitting in the single crystal Raman spectrum also reveals the influence of the intermolecular interactions. Model calculations yield an intermolecular HgF force constant of approximately 0.1 mdyn/Å. The splitting of modes, in phase motions (a_g, e_g) occur at higher wavenumbers than f_g components, is not due to repulsive interactions between states of the same symmetry. Otherwise the $\rho(CF_3)$ mode should be split e.g. by the interaction of the f_g modes $\nu_s(HgC_2)$ and $\rho(CF_3)$. Interestingly the intramolecular Hg—F distance is only 2.873(6) Å, 0.308(9) Å shorter than the intermolecular contacts. Therefore this Hg—F interaction is expected to contribute significantly to the intramolecular bonding.

According to the correlation given by Bauer et al. [2] the C—F bond length and the F—C—F bond angle are predicted from the electronegativity of the Hg atom to be 1.34 Å and 107.5°, respectively. The X-ray results are consistent with this prediction. From the vibrational spectra we conclude that gaseous (free) $Hg(CF_3)_2$ has slightly shorter C—F bonds and larger F—C—F angles than has the crystalline material.

The low CF force constant, 5.15 mdyn $Å^{-1}$, is in accord with values found for other CF_3 derivatives of electropositive elements (Table 10). The large variation of *f*(CF) indicates that this parameter is quite sensitive to changes in C—F bonding. The correlation of C—F bond distances and force constants evident from the parameters given in Table 10 should be treated with caution; no such relationship is generally valid for the currently available data on fluorocarbon compounds [13].

The HgC stretching force constant is significantly smaller in $(CF_3)_2Hg$ (2.18 mdyn $Å^{-1}$ than in $(CH_3)_2Hg$, 2.38 mdyn $Å^{-1}$ (Table 10). Even more conclusive is the comparison with the force field of CF_3HgCH_3. Here the electron-withdrawing CF_3 group strengthens the Hg—C(CH_3) bond, *f*(HgC) being essentially the same as that in CH_3HgBr [38], while in contrast, the Hg—C(CF_3) bond is further weakened by the σ-donating methyl group. The corrected Hg—C bond length in $Hg(CF_3)_2$ is 0.025(16) and 0.036(16) Å longer than that reported for $(CH_3)_2Hg$ as determined by rotational Raman [9] and electron-diffraction techniques [10], respectively. However, according to the correlation of the change in E—C(CF_3) and E—C(CH_3) bond lengths with the electronegativity of E [2], the Hg—C bond in $(CF_3)_2Hg$ should be 0.08—0.10 Å longer than that in $(CH_3)_2Hg$. Though structural data and force constants presented here prove that the Hg—C(CF_3) bond is in fact weaker than the Hg—C(CH_3) bond, the observed amount of lengthening is significantly smaller than the predicted one.

Theoretical calculations have only given qualitative interpretation of the bonding in CF_3 compounds. According to CNDO calculations [39] the ionic and covalent contributions to C—E bonding in $(CF_3)_nE$ compounds are weakened

with respect to $(CH_3)_nE$ compounds as the electronegativity of E decreases. Extended Hückel calculations attribute the relative weakening of the C—E bond to an antibonding interaction between low lying, unoccupied orbitals on E and filled orbitals localized mainly on the CF_3 group [34]. In support of this latter reasoning, the recent X-ray and vibrational spectroscopic investigations of $K[CF_3BF_3]$ revealed a "normal" B—C bond [13]. Contrary to the results of the extended Hückel calculations [34], CNDO charge distributions [39], while apparently typical for this level of theory [40], do not agree with the common opinion that the CF_3 group is more electron-withdrawing than the CH_3 group. Clearly more spectroscopic and structural data as well as more sophisticated calculations on CF_3 derivatives of electropositive elements are needed before bonding in these compounds can be fully understood.

Acknowledgement

Support by the Deutsche Forschungsgemeinschaft and the Ministerium für Wissenschaft und Forschung Nordrhein-Westfalen is gratefully acknowledged. We thank Dr. C. Krüger, Mülheim/Ruhr, for the computer drawing.

References

1 H. Bürger, G. Pawelke, A. Haas, H. Willner and A.J. Downs, Spectrochim. Acta, in press.
2 A. Yokozeki and S.H. Bauer, Top. Curr. Chem., 53 (1975) 71.
3 H. Bürger, J. Cichon, J. Grobe and F. Höfler, Spectrochim. Acta A, 28 (1972) 1275.
4 H. Bürger and R. Eujen, Spectrochim. Acta A, 31 (1975) 1645;
5 H. Bürger and R. Eujen, Spectrochim. Acta A, 31 (1975) 1655.
6 H. Bürger and R. Eujen, to be published.
7 R.J. Lagow and R. Eujen, J. Organometal. Chem., in press.
8 H.J. Emeleus and R.N. Haszeldine, J. Chem. Soc., (1949) 2953.
9 K.S. Rao, B.P. Stoicheff and R. Turner, Can. J. Phys., 38 (1960) 1516.
10 K. Kashiwabara, S. Konaka, T. Iijima and M. Kimura, Bull. Chem. Soc. Jap., 46 (1973) 407.
11 J. Mink and B. Gellai, J. Organometal. Chem., 66 (1974) 1.
12 A. Ruoff, Spectrochim. Acta A, 23 (1967) 2421.
13 D.J. Brauer, H. Bürger and G. Pawelke, Inorg. Chem., in press.
14 A.J. Downs, J. Chem. Soc., (1963) 5273.
15 I.L. Knuyants, Ya.F. Komissarov, B.L. Dyatkin and L.T. Lantsova, Izv. Akad. Nauk. SSSR, Ser. Khim., 4 (1973) 943.
16 D.J. Brauer and C. Krüger, Acta Crystallogr., B, 29 (1973) 1684.
17 J.A. Ibers and W.C. Hamilton, (Eds.), International Tables for X-Ray Crystallography, Vol. IV, The Kynoch Press, Birmingham, (1974), Table 2.2B.
18 Ref. 17, Table 2.3.1.
19 V. Schomaker and K.N. Trueblood, Acta Crystallogr. B, 24 (1968) 63.
20 C.K. Johnson and H.A. Levy, Thermal-Motion Analysis Using Bragg Diffraction Data, in ref. 17.
21 A. Bondi, J. Phys. Chem., 68 (1964) 441.
22 F. Ebert and H. Woitinek, Z. Anorg. Allgem. Chem., 210 (1933) 269.
23 D. Grdenic and C. Djordjevic, J. Chem. Soc., (1956) 1316.
24 W. Gordy and J. Sheridan, J. Chem. Phys., 22 (1954) 92.
25 J.C. Mills, H.S. Preston and C.H.L. Kennard, J. Organometal. Chem., 14 (1968) 33.
26 D.B. Crump and N.C. Payne, Inorg. Chem., 12 (1973) 1663.
27 M.R. Churchill and T.A. O'Brien, J. Chem. Soc., A, (1970) 161.
28 A.W.M. Bakke, J. Mol. Spectrosc., 41 (1972) 1.
29 G. Turrell, Infrared and Raman Spectra of Crystals, Academic Press, London, 1972.
30 P. Pulay, Gy. Borossay and F. Török, J. Mol. Struct., 2 (1968) 336.
P. Pulay and W. Sawodny, J. Mol. Spectrosc., 26 (1968) 150.
31 T. Shimanouchi, in (H. Eyring, D. Henderson and W. Jost, Eds.), Physical Chemistry, An Advanced Treatise, New York, 1970, p. 233.

32 A. Ruoff, H. Bürger and S. Biedermann, Spectrochim. Acta, A, 27 (1971) 1377.
33 H. Bürger and R. Eujen, unpublished results.
34 C.J. Marsden and L.S. Bartell, Inorg. Chem., 11 (1976) 2713.
35 G. Bouquet and M. Bigorgne, Spectrochim. Acta A, 23 (1967) 1231.
36 R.W. Kirk and P.M. Wilt, J. Mol. Spectrosc., 58 (1975) 102.
37 L.S. Bartell and L.O. Brockway, J. Chem. Phys., 32 (1960) 512.
38 P.L. Goggin and L.A. Woodward, Trans. Faraday. Soc., 62 (1966) 1423.
39 H. Oberhammer, J. Mol. Struct., 28 (1975) 349.
40 M.S. Gordon and J.A. Pople, J. Amer. Chem. Soc., 89 (1967) 4253.